7th International Conference on Biotechniques for Air Pollution Control and Bioenergy. 19th to 21st July 2017, A Coruña, Spain.

SIMULTANEOUS DISSOLVED OXYGEN AND PH CONTINUOUS MONITORING THROUGH BIOFILMS USING MINIMALLY INVASIVE MICROSENSOR

X. Guimerà[1], A. Moya[2,3], D. Rodriguez[1], D. Gabriel[4], R. Villa[2,3], A. D. Dorado[1], G. Gabriel[2,3], X. Gamisans[1]*

[1] Department of Mining, Industrial and ICT Engineering, Universitat Politècnica de Catalunya, Spain
[2] Barcelona Microelectronics Institute (IMB-CNM), CSIC, Spain
[3] Biomedical Research Networking Center in Bioengineering, Biomaterials and Nanomedicine (CIBER-BBN)
[4] Department of Chemical, Biological and Environmental Engineering, Universitat Autònoma de Barcelona, Spain
*email: xavier.gamisans@upc.edu, phone: +34938777234

www.biofiltration.cat

INTRODUCTION

The technical limitations found in the study and **monitoring of biofilms** have been solved from the design and development of a wide range of microsensors. However, available microsensors showed important limitations that have hindered a widespread use for biofiltration systems monitoring. **Microelectromechanical systems (MEMS)** technology have been used to improve microsensors design and fabrication, allowing specific design for particular applications, even biofilms monitoring. A novel microsensor have been developed based on MEMS technology: This microsensor, specially designed for biofilms profiling enables **simultaneous DO and pH monitoring along time at different biofilm locations**. The aim of this work is to show the capabilities of these microsensors for biofiltration process monitoring, obtaining **continuous microgradients** of both species within biofilms.

MICROSENSOR DEVELOPMENT

The microsensor is based on a **first prototype**, based on **oxygen amperometric** principle and designed to obtain dissolved oxygen (DO) concentration profiles of 1 mm depth via single measurement (Moya et al. 2015). The **novel prototype** (Fig. 1) was modified to **simultaneously** monitor **DO** concentration and **pH**. This device also **include** several technological **modifications** to **improve** microsensor **performance**.

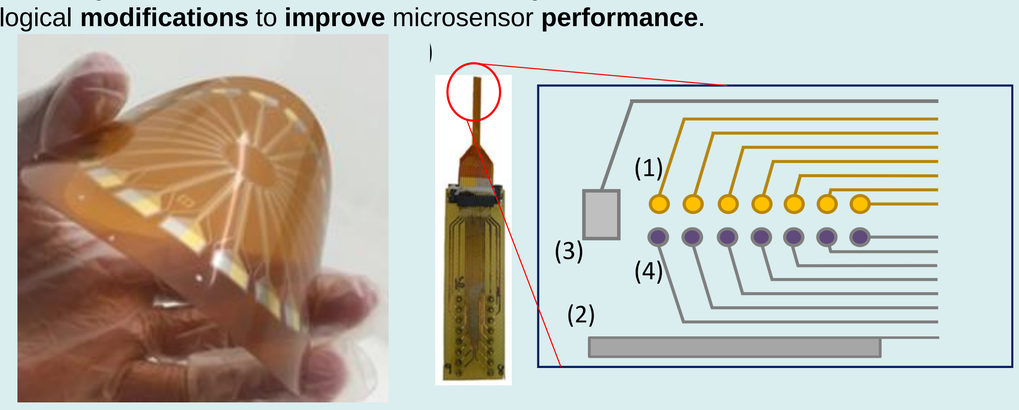

Fig 1. Microsensors wafer, ZIF connection system and needle configuration.

Technological improvements can be summarized as follow:

The **substrate** has a thickness of 125 µm, made of a flexible **Kapton** layer, in which **7 Au** electrodes (1) and **7 Pt** electrodes (4) were arranged.

Pt electrodes were coated with an **Iridium Oxide** (IrOx) layer by an electrochemical procedure for **pH monitoring**.

The **needle** includes a **Counter Electrode** (2) (CE), and a **pseudo-Reference** Electrode (pRE) (3).

Ink-Jet Printing electrodes were **coated** with a **pHEMA membrane** to avoid electrodes passivation and fouling.

SENSOR CHARACTERIZATION

Sensor response characterization: Experimental **sensitivities** were quantified at **2.06±0.08 nA·mg^{-1}·L** for DO detection, and at **61.2±0.7 mV·pH^{-1}** for pH detection.

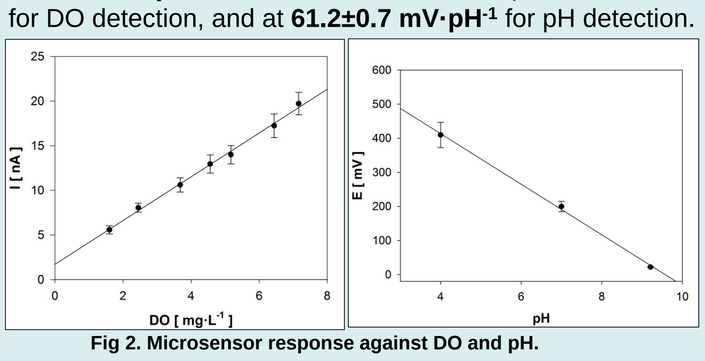

Fig 2. Microsensor response against DO and pH.

Tab 1. Detection and quantification limits for DO and pH

	L_{OD}	L_{OQ}
DO [mg·L^{-1}]	0.05 ± 0.01	0.17 ± 0.02
pH [pH units]	0.05	0.08

Besides, **pRE** and **protective membrane** ensures a **stable response** along time (Tab 2), allowing **long term measurements**. Microsensor performance for **biofilm monitoring was validated** against commercial microsensors (Fig 3).

Tab 2. DO and pH sensitivity evolution along time.

		DO sensitivity [nA·mg^{-1}·L]	pH sensitivity [mV·pH^{-1}]
Bare needle		2.06 ± 0.08	-74.2 ± 0.7
Coated needle	0 h	1.73 ± 0.12	-60.5 ± 0.6
	150 h	1.78 ± 0.14	-67.7 ± 0.6
	300 h	1.62 ± 0.08	-62.6 ± 0.6
	850 h	1.64 ± 0.16	-63.5 ± 0.6
	1000 h	1.67 ± 0.17	-62.9 ± 0.6

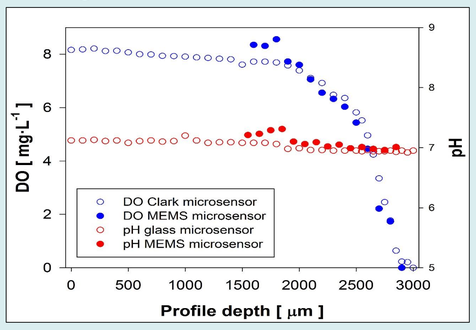

Fig 3. DO and pH profiles within biofilms.

RESULTS AND DISCUSSION

Firstly, the **developed microsensor** was employed in internal **mass transport characterization** through aerobic **biofilms**. **Diffusivity** (D_b) measurements from **oxygenation profiles** recorded by DO-MEA microsensor were conducted through an aerobic heterotrophic biofilm growth in a flat plate bioreactor (FPB). **Mass transport** was studied as **function** of biofilm **structure** along the reactor. For this purpose a **density profile** (X_b), ranging from 10 to 60 gVSS·L^{-1}, was **obtained** along the biofilm, by varying the environmental conditions such as substrate load and liquid velocity.

INTERNAL MASS TRANSPORT CHARACTERIZATION

Dynamic oxygenation profiles, used in **diffusivity determination**, were obtained from a single DO-MEA measurement. These measurements were made as is **described** in **Guimerà et al. (2015)**.
In order to obtain profiles where DO changes were only the result of **mass transport**, these profiles were conducted on **deactivated biofilms**, since diffusion through biofilms was not affected by deactivation. Bioactivity was prevented by recirculating a 300 mg·L^{-1} NaN_3 solution during 1h.

A GOOD FITTING RESULTING IN A RELIABLE ESTIMATION OF OXYGEN DIFFUSIVITY

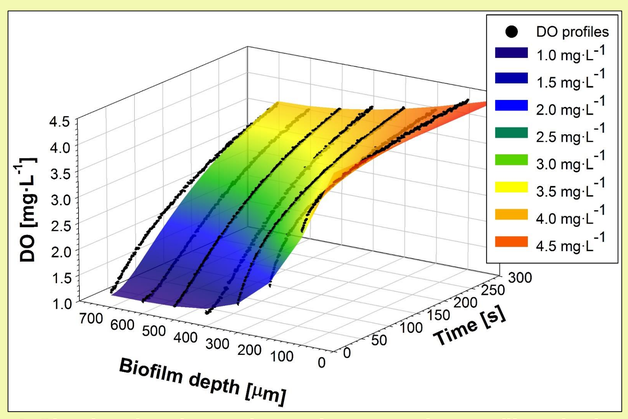

Fig 4. Simulated and experimental oxygenation profiles obtained.

The **mass transport** was described using a non-steady state diffusion model (**Fick's second law**)

$$\frac{dC}{dt} = D_B \cdot \frac{\partial^2 C}{\partial x^2}$$

Diffusivity inside **biofilms** is usually presented as **relative diffusivity** relating solute diffusivity within biofilm with the solute molecular diffusivity in water

$$D_r = D_B \cdot D_W^{-1}$$

Biofilm heterogeneity can be **introduced** into mass transport theory linking **diffusion** rate with biofilm structure, by **relating** the biofilm **diffusivity** with **biomass density**. Results revealed a clear correlation between diffusivity and biomass density within biofilms.

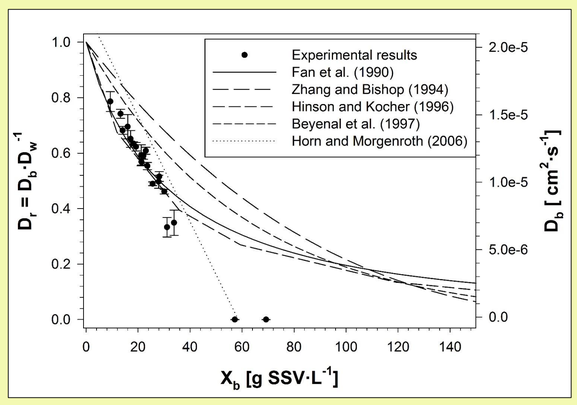

Fig 5. Biofilm diffusivities measured at different biomass densities and model correlations.

A **higher** biofilm **density** resulted in a **decrease** of biofilm porosity and thus less open volume was available to the substrate to **diffuse** through the biofilm.

CONSISTENT EXPERIMENTAL DATA FOR MASS TRANSPORT DESCRIPTION

BIOFILM MONITORING

The novel **microsensor**, based on **MEMS** technology, was **validated** for **DO** and **pH continuous monitoring** within a sulphide-oxidizing **biofilm**, grown on a gas phase biofilm reactor. During **biofilm monitoring**, gas phase residence time was reduced from 60 s to 6 s, corresponding to a **load increase** from **6 g·m^{-3}·h^{-1}** to **60 g·m^{-3}·h^{-1}**. The seven **Au**-disk electrodes were used to record **DO evolution** along time. Due to acquisition system technical limitations, **pH** could not be monitored continuously, and using IrOx coated Pt electrodes, **complete pH** profiles were acquired before and after **each load increase**.

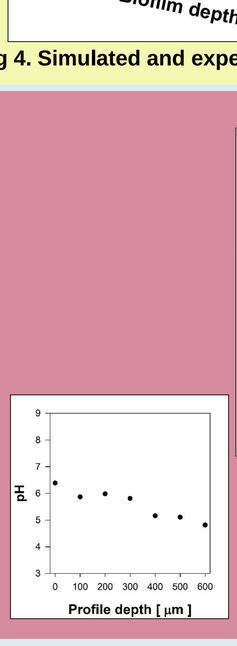

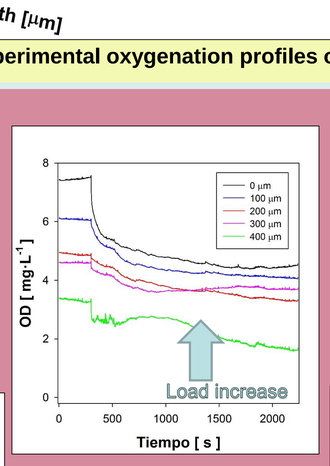

6 g·m^{-3}·h^{-1} to 12 g·m^{-3}·h^{-1}

DO MONITORING RESULTS REVEALED DIFFERENT OXYGEN CONSUMPTION VELOCITIES ALONG THE BIOFILM.

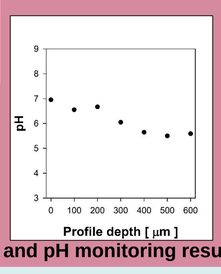

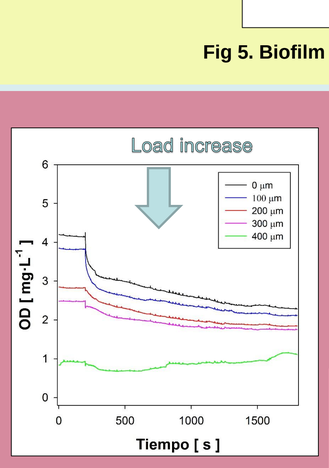

12 g·m^{-3}·h^{-1} to 48 g·m^{-3}·h^{-1}

pH DISTRIBUTION COULD NOT BE CORRELATED WITH BIOFILM ACTIVITY

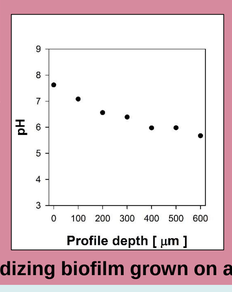

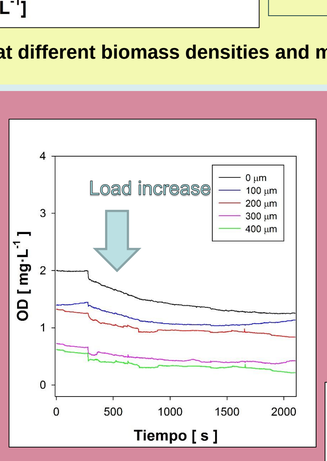

48g·m^{-3}·h^{-1} to 60 g·m^{-3}·h^{-1}

RESULTS HIGHLIGHTED THE APPEARANCE OF DO LIMITATION ZONES WHEN LOAD IS INCREASED.

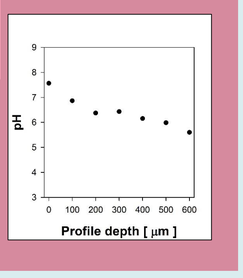

Fig 6. DO and pH monitoring results, recorded within a sulphide-oxidizing biofilm grown on a gas-phase biofilm reactor.

CONCLUSIONS

The **multi-electrode design** of the novel MEMS microsensor has **simplified** experimental **procedure** required for **biofilm profiling**, obtaining a 7-point DO and pH profile in a single measurement. **Technological modifications** have **improved** the microsensor **performance**, allowing **continuous monitoring** of **biofilm** systems. Internal **mass transport** has been exhaustively **characterized**, defining the **relationship** between **diffusion rate** and biofilm **structure**. These results **improved** mass transport **information** and description. Besides, this device allow **continuous monitoring** of biofilms, opening the possibility of **advancing** both in the **study** and **control** of **biofilms** operation.

REFERENCES

Beyenal, H., Seker, S., and Tanyolaç, A. (1997) Diffusion Coefficients of Phenol and Oxygen in a Biofilm of Pseudomonas putida. AIChE Journal, **43**(1), 243–250.
Fan, L., Wisecarver, K. D., and Zehner, B. J. (1990) Diffusion of Phenol through a Biofilm Grown on Activated Carbon Particles in a Bioreactor. Biotechnology and bioengineering, **35**, 279–286.
Guimerà, X., Moya, A., Dorado, A. D., Villa, R., Gabriel, D., Gabriel, G., and Gamisans, X. (2015) Biofilm dynamics characterization using a novel DO-MEA sensor: mass transport and biokinetics. Applied microbiology and biotechnology, **99**(1), 55–66.
Hinson, R. K. and Kocher, W. M. (1996) Model for effective diffusivities in aerobic biofilms. Journal of Environmental Engineering, **122**(November), 1023–1030.
Horn, H. and Morgenroth, E. (2006) Transport of oxygen, sodium chloride, and sodium nitrate in biofilms. Chemical Engineering Science, **61**, 1347–1356.
Moya, A., Guimerà, X., del Campo, F. J., Prats-Alfonso, E., Dorado, A. D., Baeza, M., Villa, R., Gabriel, D., Gamisans, X., and Gabriel, G. (2015) Biofilm oxygen profiling using individually addressable disk microelectrodes on a microfabricated needle. Microchimica Acta, **182**(5–6), 985–993.
Zhang, T. C. and Bishop, P. L. (1994) Evaluation of tortuosity factors and effective diffusivities in biofilms. Water Research, **28**(I), 2279–2287.

ACKNOWLEDGEMENTS

This work has been founded by the project CTQ2015-69802-C2-2-R (MINECO/FEDER, UE).